



Contents lists available at ScienceDirect

Chemical Engineering Research and Design

journal homepage: [www.elsevier.com/locate/cherd](http://www.elsevier.com/locate/cherd)iChemE  
ADVANCING  
CHEMICAL  
ENGINEERING  
WORLDWIDE

# Potential catalysts for the production of NaClO<sub>3</sub> in the decomposition of HOCl

Mária Szabó<sup>a,\*</sup>, Norbert Lihi<sup>a,c</sup>, Nina Simic<sup>b</sup>, István Fábián<sup>a,c</sup><sup>a</sup> Department of Inorganic and Analytical Chemistry, University of Debrecen, Egyetem tér 1, 4032 Debrecen, Hungary<sup>b</sup> Nouryon, SE 44580 Bohus, Sweden<sup>c</sup> MTA-DE Redox and Homogeneous Catalytic Reaction Mechanisms Research Group, University of Debrecen, Egyetem tér 1, 4032 Debrecen, Hungary

## ARTICLE INFO

## Article history:

Received 11 January 2021

Received in revised form 3 March 2021

Accepted 9 March 2021

Available online 14 March 2021

## Keywords:

Hypochlorous acid

Decomposition

Yttrium(III) chloride

Yttrium(III) oxide

Telluric acid

Chlorate process

## ABSTRACT

By pursuing the aim of identifying new types of catalysts in the electrolytic production of NaClO<sub>3</sub> from NaCl (chlorate process), we report a detailed study on the decomposition of hypochlorous acid accelerated by yttrium(III) chloride (YCl<sub>3</sub>), yttrium(III) oxide (Y<sub>2</sub>O<sub>3</sub>) and telluric acid (Te(OH)<sub>6</sub>) at 80 °C. The results were compared with those obtained in the uncatalyzed and chromium(VI) catalyzed reactions. In general, the decomposition of HOCl occurs via two competing paths toward the formation of ClO<sub>3</sub><sup>−</sup> or O<sub>2</sub>. In the case of YCl<sub>3</sub>, the decomposition proceeds via the oxygen path over the entire studied pH range. Y<sub>2</sub>O<sub>3</sub> slightly catalyzes the chlorate path under acidic conditions, however the noted catalytic effect is probably due to the “self-buffering” of the reaction mixture (Y<sub>2</sub>O<sub>3</sub> suspension). Although, a real catalytic process takes place in the presence of Te(OH)<sub>6</sub>, a significant pH-effect is also observed which is most likely associated with the acid–base equilibria of telluric acid. pH dependent studies demonstrate that the optimum pH of decomposition is at around 6.7–6.9 in this case. The comparison of the results obtained in the presence of chromium(VI) and Te(OH)<sub>6</sub> reveals that the former is a more active catalyst. On the basis of kinetic and stoichiometric results, it is reasonable to assume that Te(OH)<sub>6</sub> may be utilized as an alternative catalyst in the chlorate process.

© 2021 The Author(s). Published by Elsevier B.V. on behalf of Institution of Chemical Engineers. This is an open access article under the CC BY license (<http://creativecommons.org/licenses/by/4.0/>).

## 1. Introduction

Dichromate is an essential additive in the chlorate process (the electrolytic production of NaClO<sub>3</sub> from NaCl), to catalyze the chlorate formation as well as to inhibit side reactions. Thus, no chlorate production is possible in the current technology without adding chromium(VI) (Colman and Tilak, 1995). However, chromium(VI) compounds are in the REACH annex XIV list which means that a special authorization is required to use them within the EU after 2017. Chlorate is produced by electrolysis of sodium chloride in an undivided cell, where chlorine is produced at the anode and hydrogen at the cathode (Cornell, 2014a; Cornell, 2014b). Chlorine is

immediately hydrolyzed in the electrolyte forming hypochlorite/hypochlorous acid (their ratio is defined by the pH) which disproportionate into chlorate and chloride ions. The latter reaction is catalyzed by chromium(VI) in the electrolyte. The chromium(VI) additive has further functions in the process and large efforts have been spent to find alternative components for replacing it in all its roles in the chlorate process (Endrődi et al., 2017; Endrődi et al., 2019).

The uncatalyzed decomposition of hypochlorite has been thoroughly investigated over the years and is known to follow overall third order kinetics (Adam et al., 1992). Furthermore, the maximum rate of the reaction occurs at a pH where the ratio of HOCl and OCl<sup>−</sup> is 2:1. A deeper understanding of the mechanism of the uncatalyzed reaction was recently achieved in a theoretical study showing that the reaction is initiated by a fast equilibrium between HOCl, OCl<sup>−</sup>, Cl<sub>2</sub>O and Cl<sub>3</sub>O<sub>2</sub><sup>−</sup> and the subsequent abstraction of Cl<sup>−</sup> to form Cl<sub>2</sub>O<sub>2</sub> is the rate

\* Corresponding author.

E-mail address: [szabo.maria@science.unideb.hu](mailto:szabo.maria@science.unideb.hu) (M. Szabó).<https://doi.org/10.1016/j.cherd.2021.03.010>0263-8762/© 2021 The Author(s). Published by Elsevier B.V. on behalf of Institution of Chemical Engineers. This is an open access article under the CC BY license (<http://creativecommons.org/licenses/by/4.0/>).

determining step in chlorate formation (Szabó et al., 2018). The catalytic effect of chromium(VI) in the chlorate process has been considered for a long time, and lately this effect has been explored in detail (Endrődi et al., 2019).

Replacing chromium(VI) as a catalyst in the chlorate process is a particularly challenging task due to the extreme operating conditions applied in the corresponding technology (Endrődi et al., 2017; Sandin et al., 2015; Busch et al., 2019). In our previous work, the chromium(VI) catalyzed decomposition of HOCl was thoroughly studied, and it was concluded that the catalytically active species is  $\text{CrO}_4^{2-}$ . Such an effect was not observed with the structurally analogous phosphate ion, thus it was concluded that the catalytic activity of  $\text{CrO}_4^{2-}$  is associated with a partial electron transfer process in the transition state. This enhances the conversion of  $\text{Cl}_2\text{O}$  into  $\text{HCl}_2\text{O}_2^-$  (Kalmár et al., 2018). The main objective of this study was to find efficient alternative catalysts for the conversion of hypochlorous acid into chlorate ion. We mainly focused on compounds which were expected to feature the noted partial electron transfer phenomenon. The experiments were performed at elevated temperature ( $80^\circ\text{C}$ ) in order to mimic the process conditions.

## 2. Materials and methods

All chemicals were of analytical reagent grade, purchased from commercial sources and used as received, without further purification. Doubly-deionized and ultrafiltered (ELGA Purelab Classic system) water was used to prepare the stock solutions and samples. Sodium hypochlorite (NaOCl) solution was prepared by bubbling gaseous chlorine into sodium hydroxide solution. The stock solution of NaOCl was standardized by iodometric titration. A Metrohm 785 DMP Titrino automatic titrator equipped with a Metrohm 6.0451.100 combination platinum electrode was used. The excess NaOH concentration was determined by pH-metric titration with standard  $\text{HClO}_4$ . In this case, a Metrohm 6.0262.100 combination glass electrode was used.

The decomposition reaction was triggered by simultaneous addition of NaOCl and the catalyst to well stirred aqueous perchloric acid solution. In the case of heterogeneous systems, the progress of the reaction was monitored by taking individual samples from the reaction mixture at different reaction times, and the nominal concentration of the catalyst is given, i.e. the weighted amount of catalyst divided by the volume of the reaction mixture. Obviously, the heterogeneous catalysts were not dissolved, and the catalytic process occurred predominantly on the surface of the catalyst. The decomposition reaction was studied at  $80 \pm 0.1^\circ\text{C}$  and the samples were stirred with a magnetic stirrer. High ionic strength was not set in these experiments because it would have saturated the ion chromatographic column in the ionchromatographic experiments. Thus, the ionic strength was always defined by the ionic forms of the reactants and the catalyst in the samples. Since some of the species are involved in acid-base equilibria the actual total concentration of the ions was also affected by the pH. It follows, that constant ionic strength could not be used in these studies, it was somewhere between 0.10 and 0.15 M (estimated value). Within this range, significant ionic strength effects are unlikely on the kinetics and stoichiometry, and the corresponding results are directly comparable.

To measure the pH of the inhomogeneous reaction mixtures, a special, Metrohm Unitrode Pt 1000 (6.0258.010) electrode

was used equipped with a temperature sensor unit. Before use, it was confirmed that the electrode is reliable and reproducible in heterogeneous model systems. The electrode was calibrated every day at  $80^\circ\text{C}$  using KH-phthalate ( $c=0.05\text{ M}$ ,  $\text{pH}=4.159$ ) and borax ( $c=0.01\text{ M}$ ,  $\text{pH}=8.910$ ) standard solutions (Covington et al., 1985). In this study, the pH readout was not converted into  $\log[\text{H}^+]$  to correct for the ionic strength effect as recommended by Irving et al. (1967). Accordingly, the readout of the pH meter is plotted as pH in the corresponding figures. It needs to be emphasized that the actual correction factor (Irving factor) is electrode specific and may exceed  $\pm 1$  pH unit at  $80^\circ\text{C}$ . In principle, the correction should have been made point by point due to the lack of constant ionic strength even within a kinetic run and the presence of the heterogeneous phase. Obviously, such a procedure is not feasible. In general, the correction of the pH readout could have varied within 0.1–0.2 pH unit only.

During a kinetic run, 1 mL sample was retracted from the reaction mixture in every 5 min. This aliquot of the sample was immediately cooled to  $25^\circ\text{C}$  in an ice bath and filtrated with regenerated cellulose membrane-filter (pore size  $0.45\text{ }\mu\text{m}$ ). The filtered solution was diluted using NaOH as quenching agent. The final concentration of NaOH was 0.1 M. In the case of  $\text{YCl}_3$ , a small amount of hydroxide precipitate formed which was removed by a second filtration. UV-Vis spectra of these solutions were recorded in the 200–400 nm wavelength range on an Agilent-8453 diode array spectrophotometer. It was confirmed that unwanted photochemical side reaction did not occur during the measurements (Fábián and Lente, 2010). The amount of NaOCl was quantified at the absorption band of  $\text{OCl}^-$  ( $\lambda_{\text{max}} = 292\text{ nm}$ ,  $\epsilon = 339.5\text{ M}^{-1}\text{ cm}^{-1}$ ).

The formation of chlorate as a function of time was monitored with a Thermo Scientific Dionex ICS-5000<sup>+</sup> ion chromatographic system by using a  $25\text{ }\mu\text{L}$  injector loop. Isocratic elution was carried out using NaOH solution (0.020 M). The method was calibrated by a dilution series of chlorate solutions. In each system, the concentration of the product chlorate ion as well as the concentration change of hypochlorous acid was measured as a function of time.

The protonation constants ( $\text{pK}_a$ ) of telluric acid were determined by pH-potentiometric titration method using a carbonate free NaOH solution (ca. 1 M). The carbonate contamination was determined using the appropriate Gran functions (Gran, 1952). In this titration, 45 mL aliquots of telluric acid (ca. 0.018 M) were titrated using NaCl ( $I=1.7\text{ M}$ ) and  $\text{NaClO}_3$  ( $I=4.7\text{ M}$ ) as background electrolytes. The headspace over the sample was purged with argon to ensure the absence of oxygen and carbon dioxide. The pH measurements were made using a Metrohm Unitrode Pt 1000 (6.0258.010) electrode. In this case, the pH reading was converted to hydrogen ion concentration as described by Irving et al. (1967). The protonation constants were calculated by using the designated computational program, SUPERQUAD (Gans et al., 1985).

## 3. Results and discussion

### 3.1. General considerations

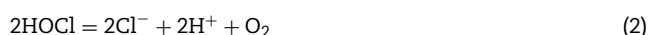
The rate of the decomposition reaction of hypochlorous acid depends on various parameters, especially on the pH. In the present study, it is assumed that the actual  $\text{pK}_a$  of HOCl is around 6.79 obtained at  $80^\circ\text{C}$ , 0.5 M NaCl (Wanngård and Wildlock, 2017). No attempt was made to determine the exact

$pK_a$  for the conditions applied here for the following reasons. The main goal of this study is to establish how various substances catalyze the decomposition of HOCl as a function of pH, but it is not studied which form of a given species is active in these reactions. Because the pH decreases steadily, the  $[OCl^-]/[HOCl]$  ratio always changes significantly over the course of the reaction. Thus, the interpretation of the general trends and the comparison of the results at different pH values does not require the exact knowledge of the  $pK_a$ . A more quantitative approach would require a different set of experiments at constant ionic strength which would not make possible the stoichiometric measurements with the method used here.

As it was reported in the case of Cr(VI) catalyzed decomposition of HOCl, the catalytic reaction path is also pH dependent (Kalmár et al., 2018). This was interpreted by considering that only one form of Cr(VI) is catalytically active and the speciation of Cr(VI) is controlled by the pH (Szabó et al., 2018). The very same features are expected in any system where the potential catalyst is involved in pH dependent equilibrium processes. The practical consequence of this is that the catalytic activity needs to be tested in a broader pH range. Thus, test experiments were run by varying the initial pH.

The kinetic traces (HOCl decay) in the presence of the potential catalyst were compared to those obtained in the Cr(VI) catalyzed reaction. The results of control experiments are also presented under identical initial conditions in either non-buffered and phosphate buffered solutions in the absence of the catalyst. The comparison of these traces revealed significant differences in the pH profiles. This is quite reasonable if we consider that different acid–base reactions and, as a consequence, different buffering effects take place in the compared systems.

Earlier it was established that the decomposition of hypochlorous acid may proceed via two distinct reaction paths (Busch et al., 2019), called the chlorate (Eq. (1)) and the oxygen (Eq. (2)) paths.



It is noteworthy to mention that only the chlorate path is preferable for the industrial process and the oxygen path needs to be avoided as much as possible. We characterize the relative significance of the two decomposition paths by the stoichiometric ratio of the reactant consumed and product formed as follows:  $R = \Delta[OCl^-]/[ClO_3^-]$ . When only the chlorate path is operative  $R = 3.0$ . Higher ratios indicate that the oxygen path also contributes to the overall process. Accordingly, the main goal is to achieve  $R = 3.0$  in a catalytic system. At this point, it needs to be emphasized that the presence of chlorate ion impurities in the reactants may have significant effect on the value of  $R$ . It was noticed that a small initial amount of chlorate ion was always present as impurity in the reaction mixtures. It could originate either from the hypochlorite stock solution or from other reagents such as perchloric acid. This problem was circumvented by fitting the kinetic traces with a polynomial function using a non-linear least squares routine to estimate the initial concentrations of HOCl and  $ClO_3^-$  (ORIGIN, 2014). In the case of HOCl, the estimated values were in excellent agreement with the values calculated by considering the dilution of the stock solutions. During the calculation of  $R$ , the measured concentration of chlorate ion was corrected by its initial concentration in each point. The uncertainties

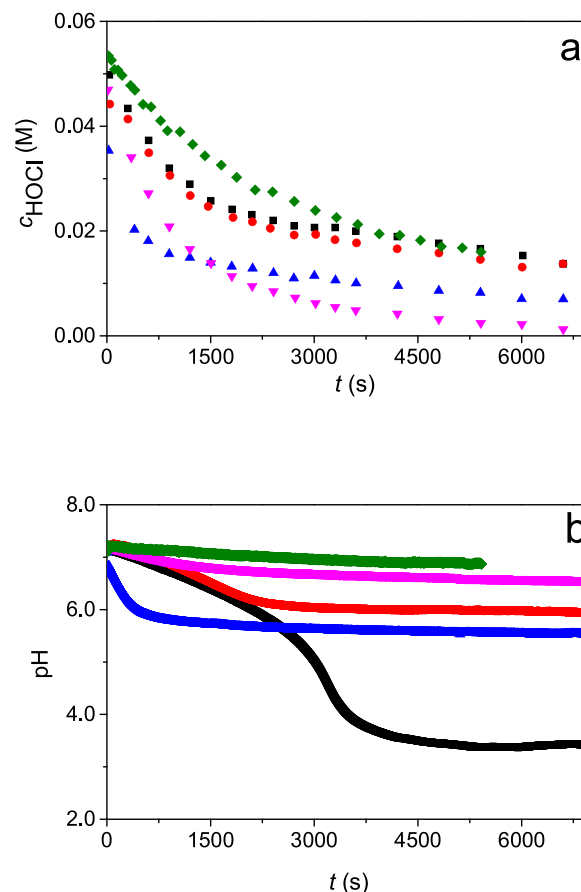


**Fig. 1 – The decay of HOCl in the absence and presence of potential catalysts (a) and the pH as a function of time during the decomposition reaction of HOCl (b). ■ control, ●  $Y_2O_3$ , ▲  $YCl_3$ , ▼  $CrO_4^{2-}$ , ◆  $PO_4^{3-}$ .  $c_{HOCl} = 0.050$  M,  $c_{cat} = 0.036$  M,  $pH_0 = 7.2$ ,  $T = 80.0$  °C.**

associated with this procedure are small and coherent results were obtained which are useful to establish the major trends in these reactions.

In agreement with the above considerations, the following requirements need to be satisfied by an ideal catalyst. It must accelerate the decay of HOCl and the catalytic process should solely progress via the chlorate path.

### 3.2. The catalytic activity of yttrium compounds

Preliminary experiments have demonstrated slight catalytic activity with  $Y_2O_3$ , therefore, we explored the role of this species and the related  $YCl_3$  in more detail. Typical chromatographic peaks of chlorate ion in the spent reaction mixtures in the absence and presence of the catalysts are shown in Fig. S1. It is quite obvious that approximately the same amounts of chlorate ion are formed in the control experiment and in the presence of  $Y_2O_3$ . The concentration of chlorate ion is considerably smaller with  $YCl_3$  which is already a strong indication that this compound promotes  $O_2$  formation.

Kinetic traces for the decomposition of HOCl at initial  $pH = 7.2$  are shown in Fig. 1. In the presence of  $YCl_3$ , the reaction is faster than in the control experiment or with  $Y_2O_3$  (Fig. 1a). In accordance with Eqs. (2) and (3), the decomposition of hypochlorous acid always generates hydrogen ion and the pH profile as a function of time strongly depends on the acid–base side-reactions in the reaction mixture (Fig. 1b). The pH drops suddenly in the control experiment at around 3000 s

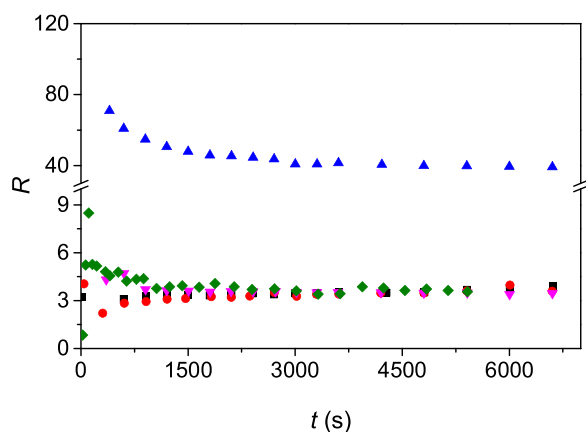


**Fig. 2 – The  $\Delta[\text{OCl}^-]/[\text{ClO}_3^-]$  ratio,  $R$ , as a function of time. ■ control, ●  $\text{Y}_2\text{O}_3$ , ▲  $\text{YCl}_3$ , ▼  $\text{CrO}_4^{2-}$ , ◆  $\text{PO}_4^{3-}$ .  $c_{\text{HOCl}} = 0.050 \text{ M}$ ,  $c_{\text{cat}} = 0.036 \text{ M}$ ,  $\text{pH}_0 = 7.2$ ,  $T = 80.0^\circ\text{C}$ .**

because the buffer capacity of the system diminishes when sufficient amount of HOCl decomposes. In the presence of  $\text{Y}_2\text{O}_3$  or  $\text{YCl}_3$ , the reaction mixtures “self-buffer” themselves to the pH 5.5–6.0 region. In the case of  $\text{YCl}_3$ , the pH decreases below 6.0 much earlier than in the other systems. This is the consequence of the hydrolysis of the catalyst which generates substantial amounts of proton. The kinetic traces in the control experiment and in the presence of  $\text{Y}_2\text{O}_3$  are identical for all practical purposes (see also Fig. S2). This confirms the lack of catalytic effects under such conditions. Phosphate ion exerts significant buffer capacity and the pH cannot decrease to the optimum range for the decomposition in the first hour. As a consequence, the reaction proceeds slower than in the control experiment. As expected on the basis of our previous studies,  $\text{CrO}_4^{2-}$  has a marked catalytic effect (Kalmár et al., 2018).

As shown in Fig. 2, the final  $R$  is around 4.0 in the control experiment and in the presence of  $\text{Y}_2\text{O}_3$ ,  $\text{PO}_4^{3-}$  and  $\text{CrO}_4^{2-}$ . In the case of  $\text{YCl}_3$ ,  $R$  is above 40 confirming that the  $\text{O}_2$ -path is dominant in the decomposition of hypochlorous. Very similar results were obtained over the entire studied pH range, i.e. when the initial pH was systematically varied from pH 7.5 to 6.15.

The actual form of Y(III) has a significant role on the overall process. When an  $\text{YCl}_3$  solution is added to the neutral or slightly alkaline reaction mixture, a gelous hydroxo precipitate forms immediately. This precipitate is presumably  $\text{Y}(\text{OH})_3$  or some sort of an oxo-hydroxo precipitate with unknown stoichiometry. The solution becomes opaque indicating the presence of a colloidal system. Accordingly, the precipitate is expected to have a relatively large specific surface area. The morphology and the surface of this precipitate are very different from that of  $\text{Y}_2\text{O}_3$ . Apparently, the surface of this precipitate is an excellent catalyst of the  $\text{O}_2$  path, similarly to the hydroxides of other metal ions such as  $\text{Ni}^{2+}$ ,  $\text{Co}^{2+}$ ,  $\text{Cu}^{2+}$ , etc. In contrast,  $\text{Y}_2\text{O}_3$  is a well-defined compound with well-defined surface structure. This may explain the difference between the catalytic activities of these compounds

### 3.3. The decomposition kinetics in the presence of $\text{Y}_2\text{O}_3$

While  $\text{Y}_2\text{O}_3$  is not an active catalyst of  $\text{O}_2$  formation, it slightly catalyzes the chlorate path under slightly acidic conditions. As shown in Fig. 3, the decomposition becomes somewhat faster in the presence of  $\text{Y}_2\text{O}_3$  when the pH is decreased.

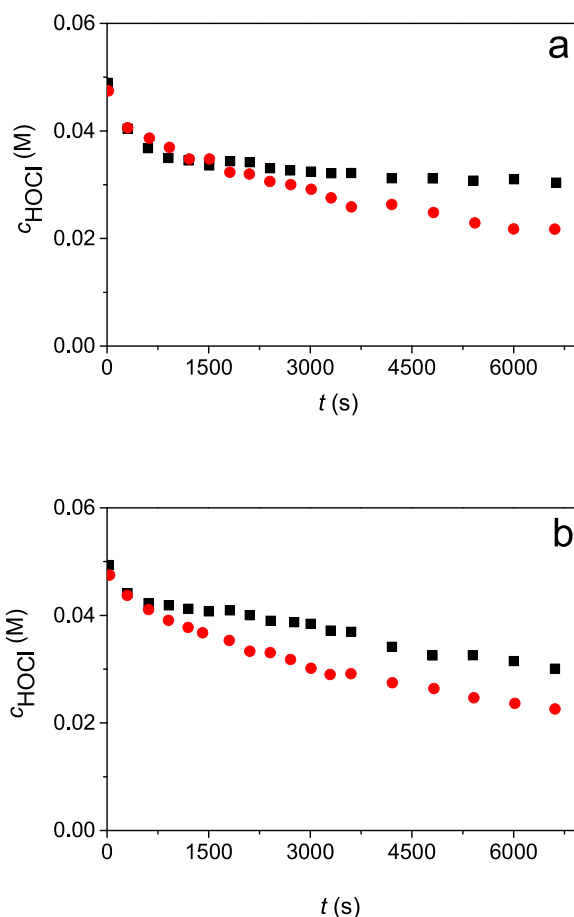


**Fig. 3 – The decay of HOCl at  $\text{pH}_0 = 6.7$  (a) and  $\text{pH}_0 = 6.2$  (b). ■ control, ●  $\text{Y}_2\text{O}_3$ .  $c_{\text{HOCl}} = 0.050 \text{ M}$ ,  $c_{\text{cat}} = 0.036 \text{ M}$ ,  $T = 80.0^\circ\text{C}$ .**

In the control experiments, the usual pH profiles were observed (Fig. S3a). As expected, the sudden pH change occurs at shorter reaction times when the initial pH is lower. The final pH is between 3 and 3.5 in all cases. In contrast, the final pH is between 5.5 and 6.0 in the presence of  $\text{Y}_2\text{O}_3$  regardless of the starting pH (Fig. S3b). This implies that  $\text{Y}_2\text{O}_3$  consumes the proton formed in the decomposition process in an acid-base reaction.

The titration of an aqueous suspension of  $\text{Y}_2\text{O}_3$  with  $\text{HClO}_4$  confirms the existence of a protonation process and, as a consequence, the appearance of a buffered region in the titration curve (Fig. S4). It should be added that the shape of the titration curve is highly dependent on the duration of the titration. Slower dosing of  $\text{HClO}_4$  results in a longer buffered region in the titration curve indicating that the acid consumption process is relatively slow. In any case, these titrations prove the origin of the buffering effect of  $\text{Y}_2\text{O}_3$  in the corresponding experiments. It is possible that the noted catalytic effect (Fig. 3) is a buffering effect in reality. It is well known that the rate of decomposition decreases by decreasing the pH below  $\text{pH} \sim 7.2$ . Thus, the reaction proceeds at higher rate in the presence of  $\text{Y}_2\text{O}_3$  because it does not allow the pH to drop suddenly.

The comparison of Fig. 4a and b confirms that the oxygen path is somewhat more pronounced in the control experiments than in the presence of  $\text{Y}_2\text{O}_3$ . It is quite apparent that the value of  $R$  increases more significantly when the starting pH of the control experiments is decreased. This leads to the conclusion that acidic conditions promote the decomposition of HOCl into  $\text{O}_2$ .



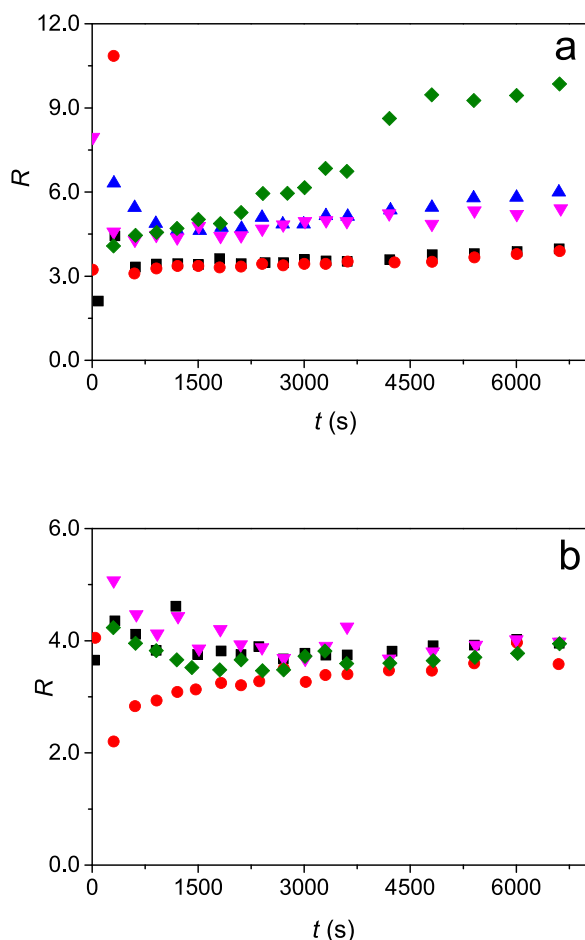


Fig. 4 – The  $\Delta[\text{OCl}^-]/[\text{ClO}_3^-]$  ratio,  $R$ , as a function of time during the control experiments (a) and in the presence of  $\text{Y}_2\text{O}_3$  (b) at different initial pH values.  $\text{pH}_0 = \blacksquare 7.5, \bullet 7.2, \blacktriangledown 6.7, \blacklozenge 6.2$ .  $c_{\text{HOCl}} = 0.050 \text{ M}$ ,  $c_{\text{cat}} = 0.036 \text{ M}$ ,  $T = 80.0^\circ\text{C}$ .

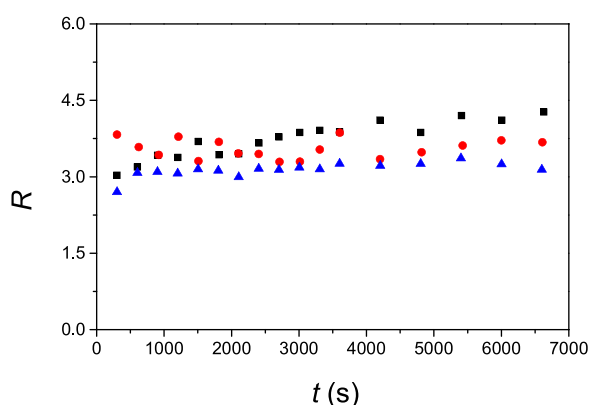


Fig. 5 – The comparison of the  $\Delta[\text{OCl}^-]/[\text{ClO}_3^-]$  ratios,  $R$ , as a function of time during the decomposition of HOCl at  $\text{pH}_0 = 6.7$ .  $\blacksquare$  control,  $\bullet \text{Y}_2\text{O}_3$ ,  $\blacktriangle \text{Te}(\text{OH})_6$ .  $c_{\text{HOCl}} = 0.050 \text{ M}$ ,  $c_{\text{cat}} = 0.036 \text{ M}$ ,  $T = 80.0^\circ\text{C}$ .

### 3.4. The catalytic activity of telluric acid

In the case of telluric acid ( $\text{Te}(\text{OH})_6$ ) remarkable results were obtained under slightly acidic conditions (Fig. S5). The kinetic traces of decomposition are compared in the presence of  $\text{Y}_2\text{O}_3$ , telluric acid and the control experiments. The results in the presence of phosphate ion are not included in the comparison because the buffer capacity of phosphate ion vanish at this relatively low pH. In the presence of telluric acid, about

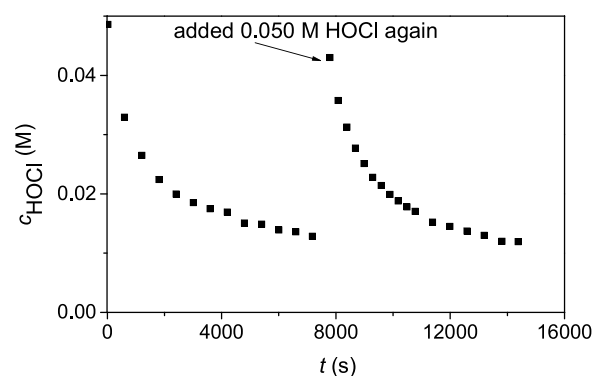


Fig. 6 – Catalytic effect of telluric acid on the decomposition of HOCl.  $c_{\text{HOCl}} = 0.050 \text{ M}$ ,  $c_{\text{cat}} = 0.036 \text{ M}$ ,  $T = 80.0^\circ\text{C}$ .

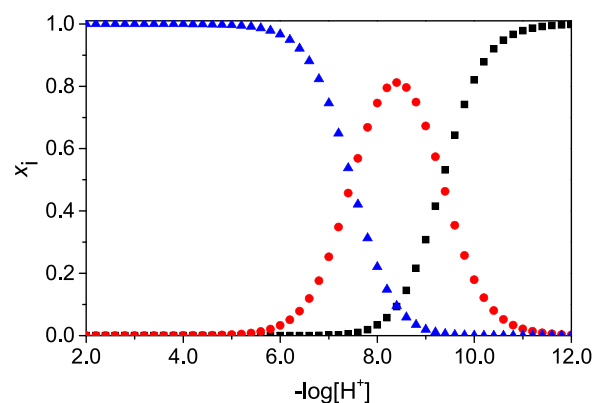


Fig. 7 – The speciation of telluric acid in aqueous solution.  $\blacktriangle \text{Te}(\text{OH})_6$ ,  $\bullet \text{TeO}(\text{OH})_5^-$ ,  $\blacksquare \text{TeO}_2(\text{OH})_4^{2-}$ .  $c_{\text{Te}} = 0.018 \text{ M}$ . ( $T = 80.0^\circ\text{C}$ ,  $I = 6.4 \text{ M NaCl} + \text{NaClO}_3$ ).

80% of the initial HOCl decomposes in about 2 h. Furthermore, the stoichiometric ratio ( $R$ ) is about 3 (Fig. 5). This excludes that the oxygen path has a significant role in this system. As shown in Fig. S6, telluric acid has a considerable buffer capacity at the studied pH, because the pH decreases only slightly compared to the control experiment. Furthermore, the acceleration of the decomposition is more pronounced with  $\text{Te}(\text{OH})_6$  than with  $\text{Y}_2\text{O}_3$  although the pH converge to about the same value at about 2 h reaction time in both cases. Thus, buffering effect alone cannot be responsible for the faster reaction and it is reasonable to assume that a real catalytic process is observed in the  $\text{Te}(\text{OH})_6$  system.

In order to explore whether decomposition is catalyzed or the oxidation of HOCl by telluric acid occurs, the following experiment was designed. First, the decomposition reaction was monitored for 2 h. After this period, an aliquot of HOCl was added to the reaction mixture bringing the HOCl concentration and the pH to the initial values. Then, the decay of HOCl was monitored again. The consecutively kinetic traces were very similar (Fig. 6), confirming that a real catalytic process takes place.

A systematic pH dependent study reveals that the optimum pH of decomposition is at somewhere around 6.7–6.9 (Fig. S7).

The noted pH effect is most likely associated with the acid–base equilibria of telluric acid. In accordance with literature results, the titration curve of acidic telluric acid solution with NaOH is consistent with two acid dissociation steps (Fig. S8). The corresponding  $\text{pK}_a$ -s are strongly dependent on the conditions applied. The speciation diagram as a function of pH was calculated by using  $\text{pK}_1 = 7.5 \pm 0.1$  and  $\text{pK}_2 = 9.3 \pm 0.1$  (Fig. 7). The estimated pH values are in

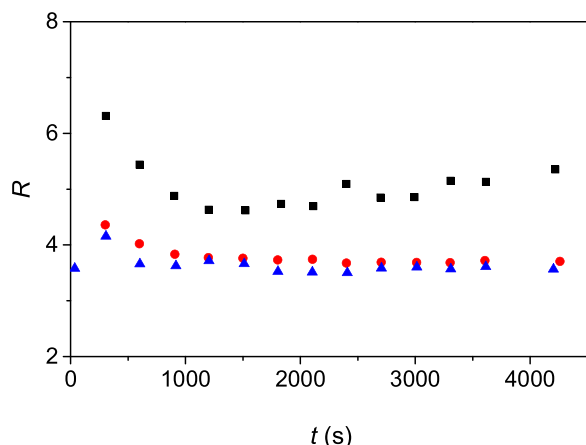


**Fig. 8** – The comparison of the  $\Delta[\text{OCl}^-]/[\text{ClO}_3^-]$  ratios,  $R$ , as a function of time during the decomposition of HOCl in the presence of Cr(VI) and telluric acid at  $\text{pH}_0 = 6.9$ . ■ control, ●  $\text{CrO}_4^{2-}$ , ▲  $\text{Te}(\text{OH})_6$ .  $c_{\text{HOCl}} = 0.050 \text{ M}$ ,  $c_{\text{cat}} = 0.036 \text{ M}$ ,  $T = 80.0^\circ\text{C}$ .

good agreement with those available in the literature (Filella and May, 2019; McPhail, 1995). The results confirm that the first deprotonation step coincides with the optimum pH region of the decomposition. This implies that somehow the  $\text{Te}(\text{OH})_6$  and  $\text{TeO}(\text{OH})_5^-$  forms are active in the catalytic process.

The comparison of the results obtained in the presence of chromium(VI) and telluric acid reveals that the former is more active catalyst (Fig. S9), but the stoichiometries of the reaction are very similar with both species (Fig. 8).

#### 4. Conclusion

The results presented here reveals that the decomposition of HOCl is clearly accelerated by  $\text{YCl}_3$ ,  $\text{Y}_2\text{O}_3$  and  $\text{Te}(\text{OH})_6$ . By comparing the stoichiometries and relative rates of the catalytic reactions, only telluric acid seems to be a useful candidate to replace Cr(VI). The comparison of the results obtained in the presence of chromium(VI) and telluric acid reveals that the former is more active catalyst, however, its adversary impact on workers health may justify the introduction of  $\text{Te}(\text{OH})_6$  as an alternative catalyst in the chlorate process. Further studies should be directed toward understanding the details of telluric acid catalysis and exploring effects of this catalyst on the electrochemistry of the industrial process. It is important to note that the higher price of the latter catalyst is an important issue regarding practical applications.

#### Declaration of interests

The authors declare that they have no known competing financial interests or personal relationships that could have appeared to influence the work reported in this paper.

#### Acknowledgements

N.L. is indebted to the New National Excellence Program of the Ministry for Innovation and Technology from the source of the National Research, Development and Innovation Fund (ÚNKP-20-4-II).

#### Appendix A. Supplementary data

Supplementary data associated with this article can be found, in the online version, at <https://doi.org/10.1016/j.cherd.2021.03.010>.

#### References

- Adam, L.C., Fábíán, I., Suzuki, K., Gordon, G., 1992. Hypochlorous acid decomposition in the pH 5–8 region. *Inorg. Chem.* 31, 3534–3541.
- Busch, M., Simic, N., Ahlberg, E., 2019. Exploring the mechanism of hypochlorous acid decomposition in aqueous solutions. *Phys. Chem. Chem. Phys.* 21, 19342–19348.
- Colman, J.E., Tilak, B.V., 1995. *Sodium Chlorate*. M. Dekker, New York.
- Cornell, A., 2014a. *Chlorate Synthesis Cells and Technology*. Springer, New York, Encyclopedia of Applied Electrochemistry.
- Cornell, A., 2014b. *Chlorate Cathodes and Electrode Design*. Springer, New York, Encyclopedia of Applied Electrochemistry.
- Covington, A.K., Bates, R.G., Durst, R.A., 1985. Definition of pH scales, standard reference values, measurement of pH and related terminology (Recommendations 1984). *Pure Appl. Chem.* 57, 531.
- Endrődi, B., Simic, N., Wildlock, M., Cornell, A., 2017. A review of chromium(VI) use in chlorate electrolysis: functions, challenges and suggested alternatives. *Electrochim. Acta* 234, 108–122.
- Endrődi, B., Sandin, S., Wildlock, M., Simic, N., Cornell, A., 2019. Suppressed oxygen evolution during chlorate formation from hypochlorite in the presence of chromium(VI). *J. Chem. Technol. Biotechnol.* 94, 1520–1527.
- Fábíán, I., Lente, G., 2010. Light-induced multistep redox reactions: the diode-array spectrophotometer as a photoreactor. *Pure Appl. Chem.* 82, 1957–1973.
- Filella, M., May, P.M., 2019. The aqueous chemistry of tellurium: critically-selected equilibrium constants for the low-molecular-weight inorganic species. *Environ. Chem.* 16, 289–295.
- Gans, P., Sabatini, A., Vacca, A., 1985. SUPERQUAD: an improved general program for computation of formation constants from potentiometric data. *J. Chem. Soc. Dalton Trans.*, 1195–1200.
- Gran, G., 1952. Determination of the equivalence point in potentiometric titrations: Part II. *Analyst* 77, 661–671.
- Irving, H.M., Miles, M.G., Pettit, L.D., 1967. A study of some problems in determining the stoichiometric proton dissociation constants of complexes by potentiometric titrations using a glass electrode. *Anal. Chim. Acta* 38, 475–488.
- Kalmár, J., Szabó, M., Simic, N., Fábíán, I., 2018. Kinetics and mechanism of the chromium(VI) catalyzed decomposition of hypochlorous acid at elevated temperature and high ionic strength. *Dalton Trans.* 47, 3831–3840.
- McPhail, D.C., 1995. Thermodynamic properties of aqueous tellurium species between 25 and 350 °C. *Geochim. Cosmochim. Acta* 59, 851–866.
- ORIGIN v. 9.1, Microcal Software Inc., Northampton, MA, 2014.
- Sandin, S., Karlsson, R.K.B., Cornell, A., 2015. Catalyzed and uncatalyzed decomposition of hypochlorite in dilute solutions. *Ind. Eng. Chem. Res.* 54, 3767–3774.
- Szabó, M., Kalmár, J., Ditrői, T., Bellér, G., Lente, G., Simic, N., Fábíán, I., 2018. Equilibria and kinetics of chromium(VI) speciation in aqueous solution – a comprehensive study from pH 2 to 11. *Inorg. Chim. Acta* 472, 295–301.
- Wanngård, J., Wildlock, M., 2017. The catalyzing effect of chromate in the chlorate formation reaction. *Chem. Eng. Res. Des.* 121, 438–447.